



Journal of Mining and Environment (JME)

journal homepage: www.jme.shahroodut.ac.ir



A New 3D Model for Shear Wave Velocity by Utilizing Conventional Petrophysical Logs and Geostatistical Method

Shahoo Maleki¹, Hamid Reza Ramazi^{1*} and Mohammad Javad Ameri Shahrabi²

1- Faculty of Mining and Metallurgical Engineering, Amirkabir University of Technology, Tehran, Iran

2- Department of Petroleum Engineering, Amirkabir University of Technology, Tehran, Iran

Article Info

Received 7 December 2022

Received in Revised form 19 April 2022

Accepted 8 May 2022

Published online 8 May 2022

DOI:10.22044/jme.2022.11462.2134

Keywords

3D model

Estimation

Kriging estimator

Well logs

Shear wave velocity

Abstract

Shear wave velocity (V_s) is considered as a key parameter in determination of the subsurface geomechanical properties in any hydrocarbon-bearing reservoir. During a well logging operation, the magnitude of V_s can be directly measured through the dipole shear sonic imager (DSI) logs. On a negative note, this method not only is limited to one dimensional (1D) interpretation, it also appears to be relatively costly. In this research work, the magnitude of V_s is calculated using one set of controversial petrophysical logs (compressional wave velocity) for an oil reservoir situated in the south part of Iran. To do this, initially, the pertinent empirical correlations between the compressional (V_p) and shear wave velocities are extracted for DSI logs. Then those empirical correlations are deployed in order to calculate the values of V_s within a series of thirty wells, in which their V_p values are already recorded. Afterwards, the Kriging estimator along with the Back Propagation Neural Network (BPNN) technique are utilized to calculate the values of V_s throughout the whole reservoir. Eventually, the results obtained from the two aforementioned techniques are compared with each other. Comparing those results, it turns out that the Kriging estimation technique presents more accurate values of V_s than the BPNN technique. Hence, the supremacy of the Kriging estimation technique over the BPNN technique must be regarded to achieve a further reliable magnitude of V_s in the subjected oil field. This application can also be considered in any other oil field with similar geomechanical and geological circumstances.

1. Introduction

Some of the petrophysical well log data acquired in the exploration phase of a hydrocarbon reservoir can provide precious information about the behavior of the reservoir geomechanics. The compressional wave velocity (V_p) logs and Shear wave velocity (V_s) are the petrophysical well logs for well logging tools. The V_p logs can be obtained by sonic logging that is usually available for all wells in the hydrocarbon reservoir fields. Nevertheless, the V_s logs can only be obtained by utilizing the dipole shear sonic imager (DSI) logs that is not available for all wells in the hydrocarbon reservoir fields because measurement of this data logs is more complicated and very expensive. Consequently, many researchers have tried to solve

these problems by means of empirical equations [1-19]. For this means, the empirical method has directly been determined by the DSI logs, which is a quantitative formulation between the V_s logs data from the DSI logs and other logs data from the conventional petrophysical logs data. Due to that, the empirical equations in a field depend on the geological and tectonic reservoir conditions as well as the type of conventional well logs available; if the condition and well logs are not similar and existing, these equations cannot satisfactorily be applied to other wells or fields. Hence, the geophysical and geomechanical researchers have tried to remove this weakness by replacing the artificial intelligence methods. For example,

✉ Corresponding ramazi@aut.ac.ir (H.R. Ramazi).

Behnia et al [19] by using gene expression programming (GEP), and neuro-genetic and adaptive neuro-fuzzy inference system (ANFIS) have predicted the shear wave velocity in the limestone reservoir. The results obtained showed that the ANFIS method was the best predictor that could be used in the prediction of shear wave velocity. Moreover, in the past decade, other artificial intelligence approaches have been used to estimate the shear wave velocity that has shown better results than the empirical methods [e.g., 20-24,17,18]. From the past to the present time, all the methods that have been presented to determine shear wave velocity are the extrapolation and empirical methods. Owing to the fact that the geological and tectonic properties in the different places of a hydrocarbon reservoir filed and diverse reservoir filed are variable, these methods cannot be considerably accurate in a large scale.

In the past few decades, the geostatistical estimation and simulation methods have commonly been used in the earth science that have been successfully applied to determine diverse parameters [see, e.g., 25-34]. Among the methods that have been introduced so far, in many cases, the Kriging method has provided more acceptable results than the other methods. Kriging is a geostatistical interpolation method for optimal spatial estimation [35]. This method provides a solution to the problem of estimation based on a continuous model of stochastic spatial variation, and takes the variogram model [36]. It is an estimation method that gives the best unbiased linear estimates of point values or of block averages [37]. Three types of linear kriging estimators have been widely used in the earth science, which include ordinary kriging (OK), used when the mean is unknown, Simple Kriging (SK), used when the mean is known, and the mean value kriging, used to estimate the value of the mean when it is unknown [38, 39].

The aim of this research work is to use the kriging estimators and well logs data belonging to an onshore oil field for estimating the shear wave velocity in overall a carbonate reservoir.

2. Geology of Studied Area

This work uses the data belonging to an onshore oil field that is located in the Province of Khuzestan, Abadan plain, near the Iran-Iraq frontier. The Abadan plain including this oil field structure is situated within the Mesopotamian foredeep basin in the SW of the Zagros foreland. Prior to the final collision of the oceanic domain between the continents had been under convergence at least since the late Eocene time. The Zagros foreland basin comprises the synand post-Zagros collision succession (upper Miocene to Holocene), which together with the deeper units (i.e. post Permian succession), has been deformed by the subsequent folding and thrusting. The foredeep basin area contains many super-giant oil and gas fields (see Figure 1). This case study oil field structure is around 23 km in length and 9 km wide. The trend of the structure is an exception to the belt of foothill fold of southwestern Iran, striking NW-SE. Regional unconformities were present at the top of Dariyan, Sarvak, Gurpi, and Jahrum, and they showed the effect of epirogenic movements. Above the Tarbour Member (inside Gurpi Formation), there is no structural closure, and it seems that this area is tilted to NE due to the Zagros orogeny.

The Fahliyan Formation is well-exposed in the Zagros Mountains, in the Fars Province [40]. At the same time of the sedimentation of the Fahliyan, in the area located between the oilfield and the Khuzestan Province, the intra-shelf basin of the Garau Formation takes place. The current oilfield area at the time of the Fahliyan sedimentation must belong to an articulate carbonate ramp complex, partly controlled by local tectonics, partly by sea level changes, probably limited Eastward by a more subsiding area underwent a deeper sedimentation. Argillaceous limestones and shales of deep environment also develop in Offshore Kuwait, suggesting that this area belonged to the same intra-shelf basin. The sedimentation of these units is related to the significant sea level rise started during the late Tithonian and continued into the early Berriasian [41]. The shallow water sequences of Fahliyan and equivalent units of northern Persian Gulf underlay the shale and bioclastic limestone of the Ratawi Formation.



Figure 1. Geographical location of oil and gas fields in the Zagros foredeep basin.

3. Well logging data

The well logging data of this research work belongs to a number of thirty (30) vertical wellbores drilled into a carbonate reservoir situated in the southwestern part of Iran. The digitized well logs consist of the V_s data from DSI logging in one well, and the V_p data from sonic logging in the thirty wells. Figure 2 shows the plot of the well logging data from DSI and petrophysics logs that have been used to find the relationship between the V_p and V_s logs in this work. As shown in Figure 2, a number of nine well logs including the Density log (ROHB), Caliper log (CAL), Shear wave

velocity (V_s), Compression wave velocity (V_p), Gamma ray log (GR), True formation Resistivity log (RT), Total porosity (PIGT), Temperature (TEMP), and Poisson's Ratio (PR) have been used. Each one of the well logs contained 1562 records along the depth range of 4304-4542 m. Furthermore, a number of 99892 V_p logs data from the thirty vertical wellbores in the different depths were recorded, and were adopted in this research work. For all the well logs data, the statistical characteristics such as percentile values, central tendency, dispersion, and distribution were calculated. The corresponding results are shown in Table 1.

Table 1. Statistical characteristics for well logs data.

N	Valid	PR 1562	RHOB 1562	GR 1562	RT 1562	CAL 1562	PIGT 1562	TEMP 1562	V_p 1562	V_s 1562
Mean		0.301363	0.999035	25.45516	389.9904	6.204865	0.102544	134.9058	0.016267	0.008741
Std. error of mean		0.000555	1.29E-05	0.23479	87.80941	0.020698	0.001612	0.058219	5.84E-05	2.86E-05
Median		0.2979	0.999035	23.1291	59.49143	5.8554	0.110265	134.9057	0.015413	0.008436
Mode		0.2935	0.998154	20.6828	0.54564	5.7711	0.01677	130.9243	0.014774	0.007239
Std. deviation		0.021928	0.000509	9.279399	3470.416	0.818015	0.063715	2.300934	0.002306	0.001129
Variance		0.000481	2.59E-07	86.10724	12043789	0.669148	0.00406	5.294296	5.32E-06	1.27E-06
Skewness		-1.49779	7.81E-14	1.333179	25.83176	2.917466	-0.05354	1.24E-06	0.473953	0.582845
Std. error of skewness		0.061918	0.061918	0.061918	0.061918	0.061918	0.061918	0.061918	0.061918	0.061918
Kurtosis		17.35062	-1.2	1.92978	703.0447	12.33003	-1.19039	-1.2	-1.24481	-0.68928
Std. error of kurtosis		0.123758	0.123758	0.123758	0.123758	0.123758	0.123758	0.123758	0.123758	0.123758
Range		0.3169	0.001761	55.9956	99999.45	6.4587	0.30237	7.96299	0.007886	0.00541
Minimum		0.0626	0.998154	9.0195	0.54564	5.6562	0.00368	130.9243	0.012714	0.006869
Maximum		0.3795	0.999915	65.0151	100000	12.1149	0.30605	138.8873	0.020601	0.012278
Percentiles	25	0.2887	0.998594	19.2294	32.19631	5.7711	0.0327	132.9125	0.014331	0.007766
	50	0.2979	0.999035	23.1291	59.49143	5.8554	0.110265	134.9057	0.015413	0.008436
	75	0.3145	0.999476	29.3435	131.6916	6.0852	0.153028	136.8991	0.018562	0.009627

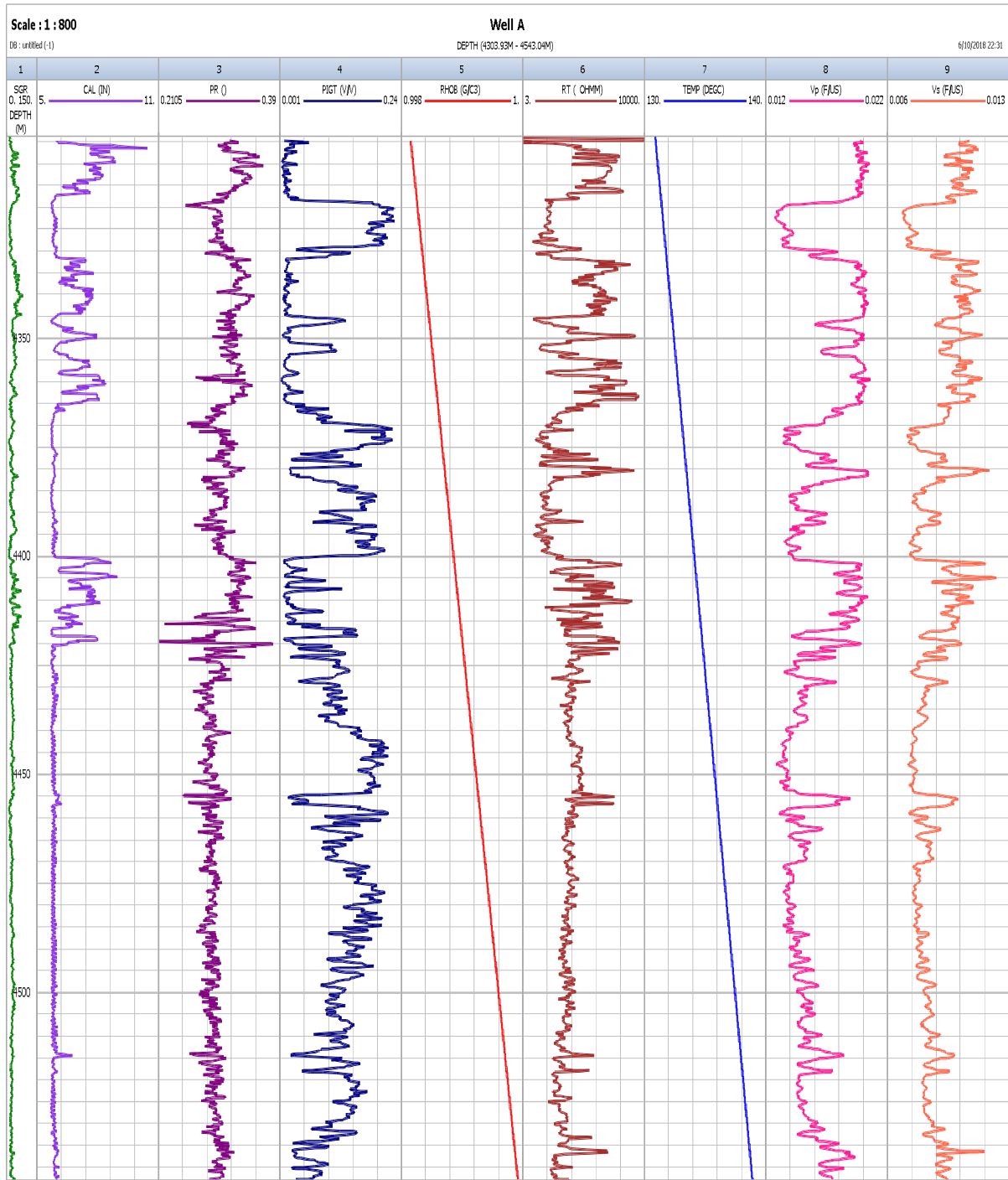


Figure 2. Applied well logging data.

To understand the relationship of dependency between the V_s and V_p logs data, firstly, the V_s and V_p data was obtained from the DSI logs, and then

the scatter plot was drawn. Furthermore, the best linear regression line was fitted on this data (Figure 3).

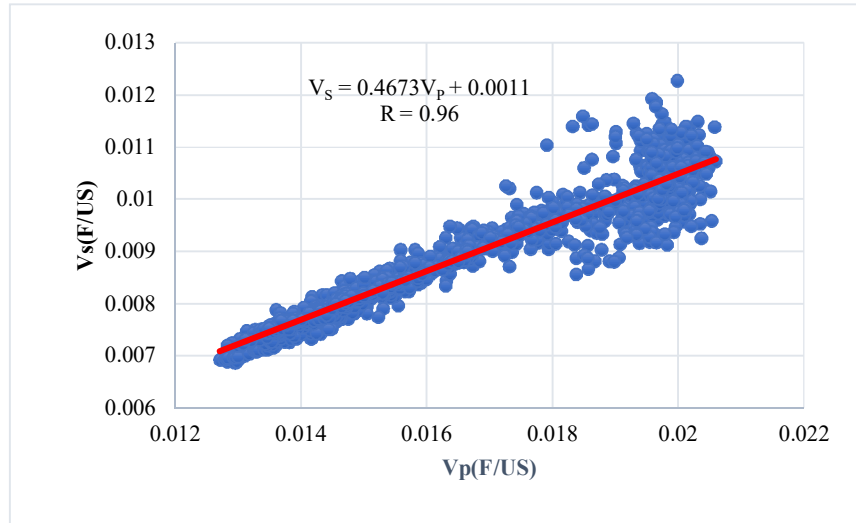


Figure 3. Scatter plot showing relationship of dependency between V_s and V_p logs data.

Figure 3 shows that there is an acceptable correlation between the V_s and V_p logs data in the subjected field. Consequently, the equation of linear regression that was derived from the scatter plot was used to estimate the V_s logs data in the other wells, which V_p logs data was obtained from the sonic logging. Therefore, the linear equation between the V_s and V_p logs data was found as:

$$V_s = 0.001281 + 0.4584V_p \quad (1)$$

where V_s and V_p are the shear and compressional wave velocities, respectively. In this equation, the unit of V_s and V_p is $ft / \mu s$.

As already mentioned, for the thirty wells in the reservoir intervals, there is an amount of compressional wave velocity. So that by utilizing the above equation (Eq. (1)), the shear wave velocity in those wells was calculated (Figure 4).

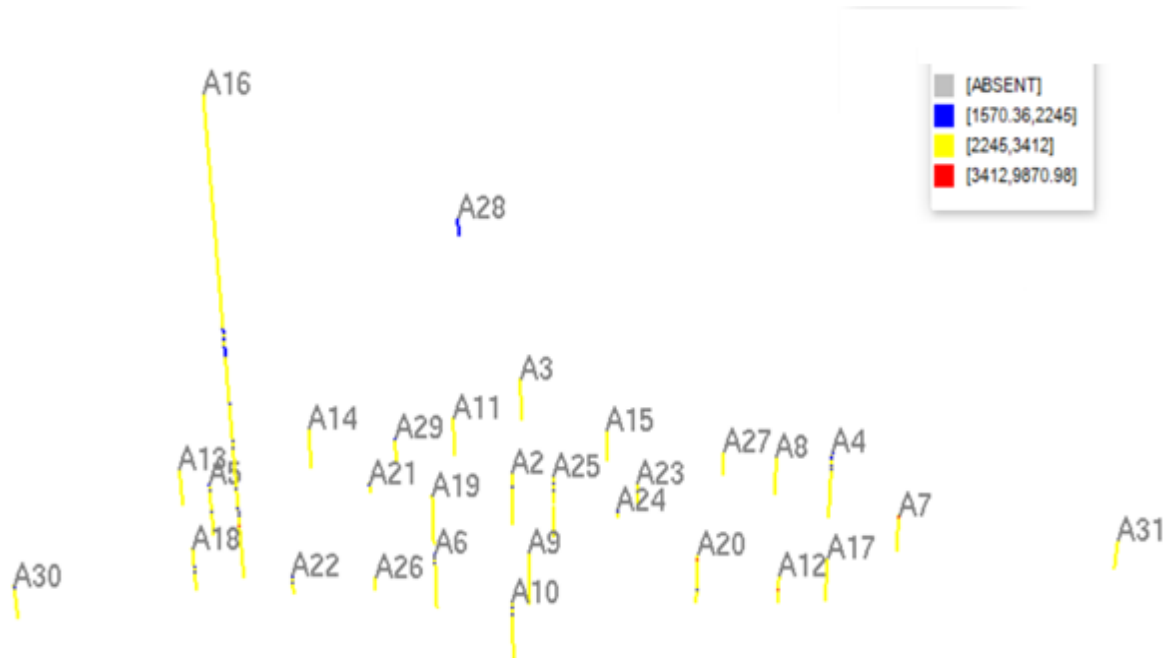


Figure 4. Shear wave velocity data in the thirty wells.

4. Methodology

4.1. Back-Propagation Neural Network

The purpose of applying Artificial Neural Network (ANN) is to extend a mathematical model of biological events in order to imitate the capability of biological neural structures for designing an intelligent information processing system [17]. Back-propagation neural network (BPNN) is an active scientific approach due to the efficiency in the modeling non-linear dynamic systems [17, 42]. A range of numerous applications can be found in various papers indicating the ability of this typical neural network [17, 43]. BPNN is usually recognized for its prediction capability to generalize well on a wide variety of problems. For example, Liang and Gupta have studied the stability of dynamic back-propagation training algorithm by the Lyapunov method [17]. This network is a supervised approach that means that it must be trained with both the input and target output data. During the training process, the network tries to match the outputs with the desired target values. Learning starts with the assignment of random weights. The output is then calculated, and the error is estimated [17]. This error is used to update the weights until the stopping criterion is reached. It should be noted that the stopping criterion is usually the average error of epoch [17].

4.2. Geostatistics Estimation

Geostatistical analysis are a branch of classical statistics that are widely used to determine the spatial correlations between variables. In the nature, when sample points are approximately near to each other, the difference between a measured value of a parameter in these points is insignificant,

but as the points distances increase, the difference increases too, which suggests measured values of the same parameter changed intensively [34]. This phenomenon is a signature implicating of the space effects on parameters values [34]. Therefore, geostatistics is an interpolation method that uses the space location between points to determine the unknown values from an estimated parameter. This instrumental capability presented geostatistics as a powerful method in making the reliable three-dimensional models of various properties [34, 44-46]. In the petroleum science and engineering, this work objects at interpretation of geology, geophysics and reservoir modeling [46]. There are different methods to determine the space distribution of a variable in geostatistics. For example, today, kriging method is one of the most practical methods in geostatistics. Kriging is an estimation method that gives the best unbiased linear estimates of point values or of block averages [37]. There are different types of kriging estimators, but in here only ordinary kriging (OK) to be introduced. OK used when the mean is unknown and defined as follows:

The variable $Z(x)$ is assumed to be stationary with mean m . Its mean at every point is equal to m and so is the mean of any block [37]. That is,

$$E[Z(x_i)] = m, \quad E(Z_V) = m \tag{2}$$

Most estimators are weighted moving averages of the surrounding data values; that is, they are linear combinations of the data:

$$Z_V^* = \sum \lambda_i Z(x_i) \tag{3}$$

Condition of unbiasedness is as follows:

$$E [Z_V^* - Z_V] = E [\sum \lambda_i Z(x_i) - Z_V] = \sum \lambda_i m - m = m [\sum \lambda_i - 1] \tag{4}$$

In order to be unbiased, the expected error must be zero, so either $m=0$ or the kriging weights must add up to 1. The variance of the error estimation

can be expressed in terms of either the covariance or the variogram [37]:

$$\begin{aligned} Var [Z_V^* - Z_V] &= \sum \sum \lambda_i \lambda_j C(x_i, x_j) + \bar{C}(V, V) - 2 \sum \lambda_i \bar{C}(x_i, V) \\ &= 2 \sum \lambda_i \bar{\gamma}(x_i, V) - \sum \sum \lambda_i \lambda_j \gamma(x_i, x_j) - \bar{\gamma}(V, V) \end{aligned} \tag{5}$$

where $\bar{\gamma}(V, V)$ is the average of the variogram between any two points x and x' sweeping independently throughout the volume V .

$$\bar{\gamma}(V, V) = \frac{1}{V^2} \int \int \gamma(x - x') dx dx' \quad (6)$$

Equation 6 explains the block kriging. When the uncertainty is relatively large, one might want to smooth the interpolated results by performing kriging on a larger area than single points. This type of kriging interpolation is known as block kriging.

In the same way $\bar{C}(x_i, V)$ and $\bar{C}(V, V)$ are the averages for the covariance. In order to minimize

the estimation variance under the constraint that the sum of the kriging weights must be equal to 1, a Lagrange multiplier μ has been introduced into the expression to be minimized [37]. The problem is minimized by the following equation:

$$\phi = Var(Z_v^* - Z_v) - 2\mu(\sum \lambda_i - 1) \quad (7)$$

The partial derivatives of the quantity are then set to zero. This leads to a set of $N+1$ linear equations called the kriging equations or kriging system. When written these equations in terms of the variogram model the kriging system is [37]:

$$\begin{cases} \frac{\partial \phi}{\partial \lambda_i} = 0 \Rightarrow \sum_{j=1}^N \lambda_j \gamma(x_i, x_j) + \mu = \bar{\gamma}(x_i, V) & i = 1, 2, \dots, N \\ \frac{\partial \phi}{\partial \mu} = 0 \Rightarrow \sum_i^N \lambda_i = 1 \end{cases} \quad (8)$$

The minimum of the variance which is called the kriging variance, is given by [37]:

$$\sigma_K^2 = \sum \lambda_i \bar{\gamma}(x_i, V) - \bar{\gamma}(V, V) + \mu \quad (9)$$

Moreover, the equations could also have been obtained in terms of the covariance by minimizing the first form of equation 4. The kriging system is as follows [37]:

$$\begin{cases} \sum_{j=1}^N \lambda_j C(x_i, x_j) + \mu' = \bar{C}(x_i, V) & i = 1, 2 \dots N \\ \sum_i \lambda_i = 1 \end{cases} \quad (10)$$

The two Lagrange multipliers are related by $\mu = \mu'$. The corresponding kriging variance is given by [37]:

$$\sigma_K^2 = \bar{C}(V, V) - \mu - \sum \lambda_i \bar{C}(x_i, V) \quad (11)$$

To solve the numerical system, it is convenient to write it in matrix form: $AX = B$ [37].

$$\begin{bmatrix} \gamma_{11} & \gamma_{12} & \dots & \gamma_{1N} & 1 \\ \gamma_{21} & \gamma_{22} & \dots & \gamma_{2N} & 1 \\ \cdot & \cdot & \cdot & \cdot & \cdot \\ \gamma_{N1} & \gamma_{N2} & \dots & \gamma_{NN} & 1 \\ 1 & 1 & \dots & 1 & 0 \end{bmatrix} \begin{bmatrix} \lambda_1 \\ \lambda_2 \\ \cdot \\ \cdot \\ \lambda_N \\ \mu \end{bmatrix} = \begin{bmatrix} \bar{\gamma}(x_1, V) \\ \bar{\gamma}(x_2, V) \\ \cdot \\ \cdot \\ \bar{\gamma}(x_N, V) \\ 1 \end{bmatrix} \quad (12)$$

If γ is an admissible model and if there are no multiple points, the matrix A is always non-

singular. Its inverse A^{-1} exists. So a solution exists and it can be proved that it is unique [37].

$$X = A^{-1}B \quad (13)$$

The kriging variance can be written:

$$\sigma_k^2 = X^T B - \bar{y}(V, V) \quad (X^T = X \text{ transpose}) \quad (14)$$

Note that the matrix A itself is not positive definite.

5. Results and Discussion

5.1. Back-Propagation Neural Network

In this study, shear wave velocity was estimated by BPNN method and coordinate data (X, Y and Z). To do this firstly, the actual data of shear wave

velocity was derived by DSI logs in only one well (well A), and then, those data logs along with the coordinate data (X, Y, and Z) were used to estimate the shear wave velocity of BPNN. The data set was divided into the training and testing data with a ratio of 70% to 30%, respectively. In this case, the optimum networks included one input layer consisting of 3 neurons (X, Y, Z), three hidden layers of sigmoidal function comprising 8, 5 and 2 neurons, and an output layer containing only one neuron (S-wave velocity). The predicted values for the shear wave velocities using the BPNN algorithms versus the real values are shown in Figure 5.

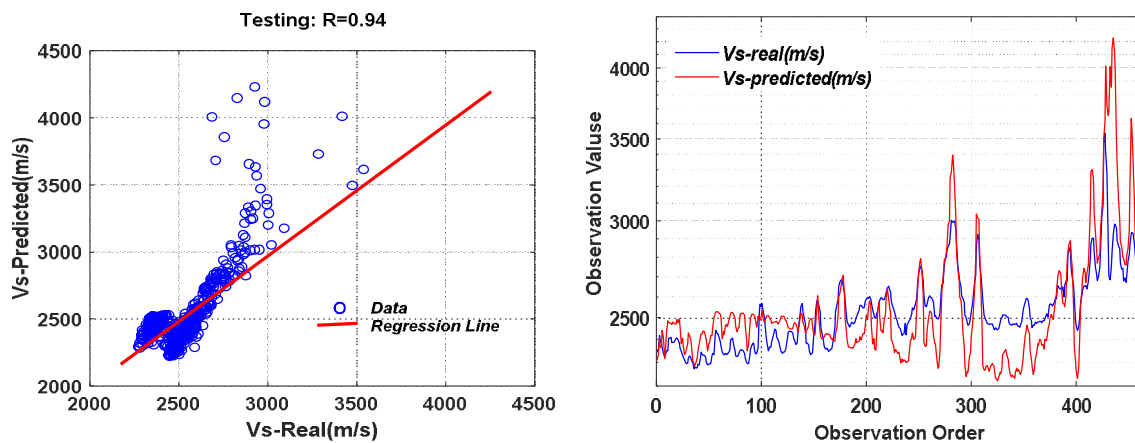


Figure 5. Demonstrating real V_S versus predicted V_S (left) and errors of V_S estimation using BPNN for well A (right).

As it can be seen, in Figure 5, the results show a relatively good coefficient of determination ($R = 0.94$), whereas the estimation process (error) is not more accurate.

Then the BPNN code was run for thirty shear wave velocity datasets, which were previously shown in Figure 4. In this case, the input datasets were the coordinates (X, Y, Z), the hidden layers were three layers of sigmoidal function comprising 8, 5, and 2 neurons, and the output was the shear wave velocity with the ratio of training to test data equal as 70% to 30%, just like we did in the previous case. The results obtained are shown in Figure 6.

The results obtained in Fig. 6 show a low correlation coefficient of determination ($R = 0.32$), and a high error for the determined shear wave velocity. Therefore, this method is not appropriate in the estimation of shear wave velocity.

5.2. Geostatistics Estimation

5.2.1. Variography Results

In geostatistics, a spatial structure is necessary, which is expressed by the variogram model. Variogram is a basic tool for investigating the spatial structure. Kriging is the geostatistical estimator used in this research work. As it was previously mentioned, the variogram model is a critical parameter for various Kriging estimators. Therefore, the exactitude of the offered parameters from the variogram is of crucial significance and it can have a significant, positive (or negative) influence on the estimated blocks [39, 47]. The variogram provides an understanding of spatial mutability of a property versus the distance; its value increases as single values of a sample become more diverse [48]. One of the most important conceivable deployments of variogram is the estimation of the parameter value at the unsampled location, and/or estimation of the average over a certain area [49]. In this research work, in order to create a 3D model by the Kriging method

for the oil field, firstly, the variography was carried out. This work was conducted through the Datamine software, which is a reliable in geo-statistics estimation. Then in order to create the variogram, the records of shear wave velocity data

in the 30 wells were used. This data was already shown in Figure 4. Correcting these datasets, their wireframes were plotted, and after applying wireframes, the additional shear wave velocity data was removed (Figure 7).

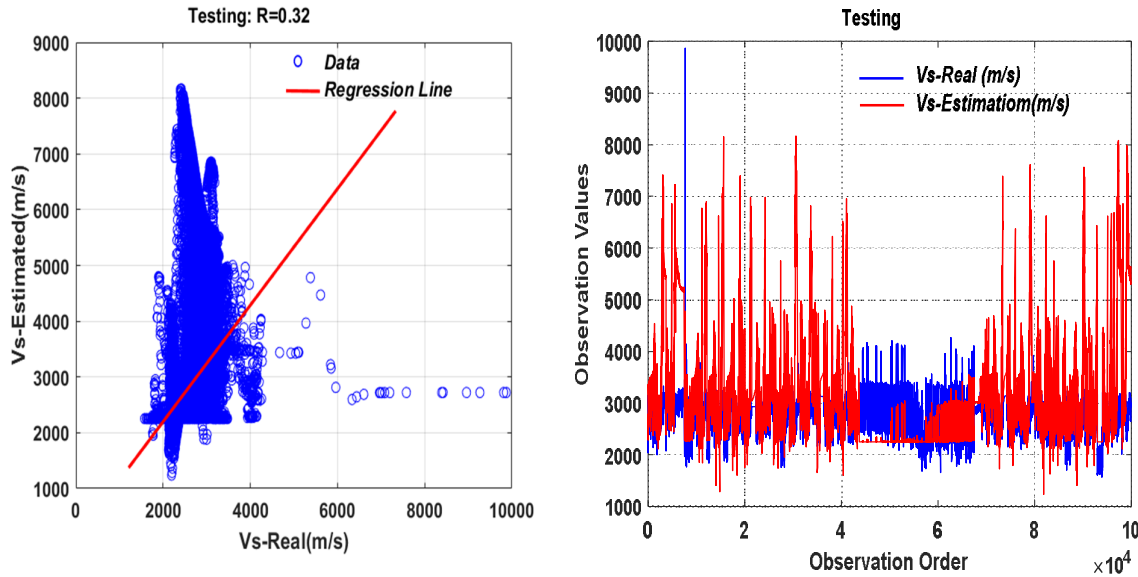


Figure 6. Demonstrating real versus predicted shear wave velocity (left) and errors of shear wave velocity estimation using BPNN (right) for thirty wells.

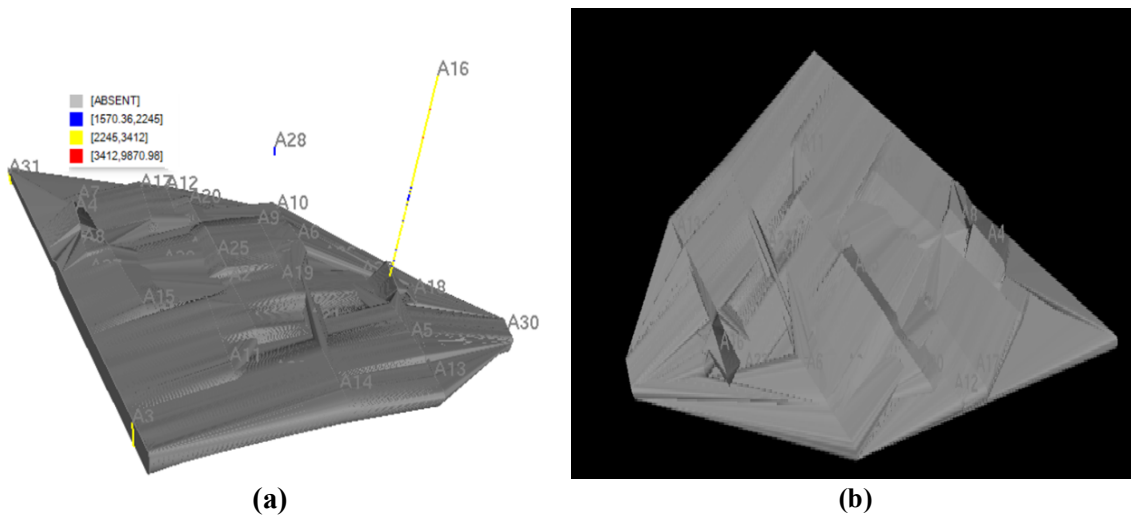


Figure 7. Shear wave velocity wireframes for 30 wells in reservoir intervals (before (a) and after (b) applying corrections with wireframes).

In the next step, the experimental variograms were performed on the shear wave velocity data from the wireframes. According to the anisotropy of the reservoir, three perpendicular variograms were required to determine the appropriate

elliptical search area. Therefore, the variograms for different parameters such as azimuth and dip were determined, and eventually, the suitable theoretical models based on the least square differences were fitted to them (see Figures 8 to 10).

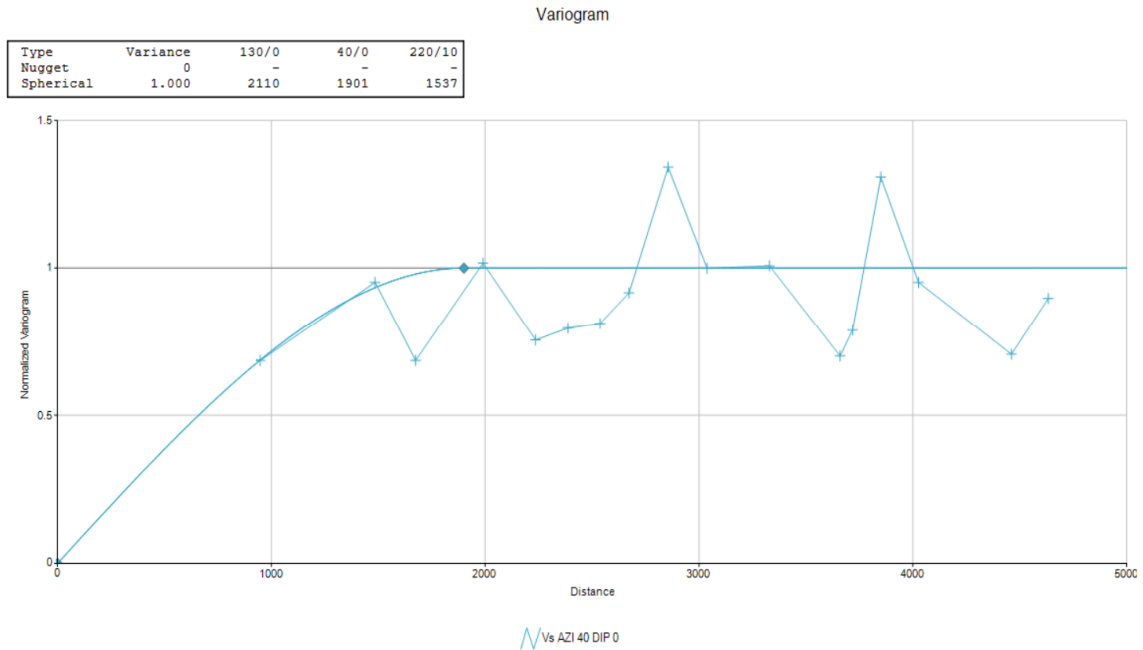


Figure 8. Variogram model for shear wave velocity in azimuth 40 and dip 0.

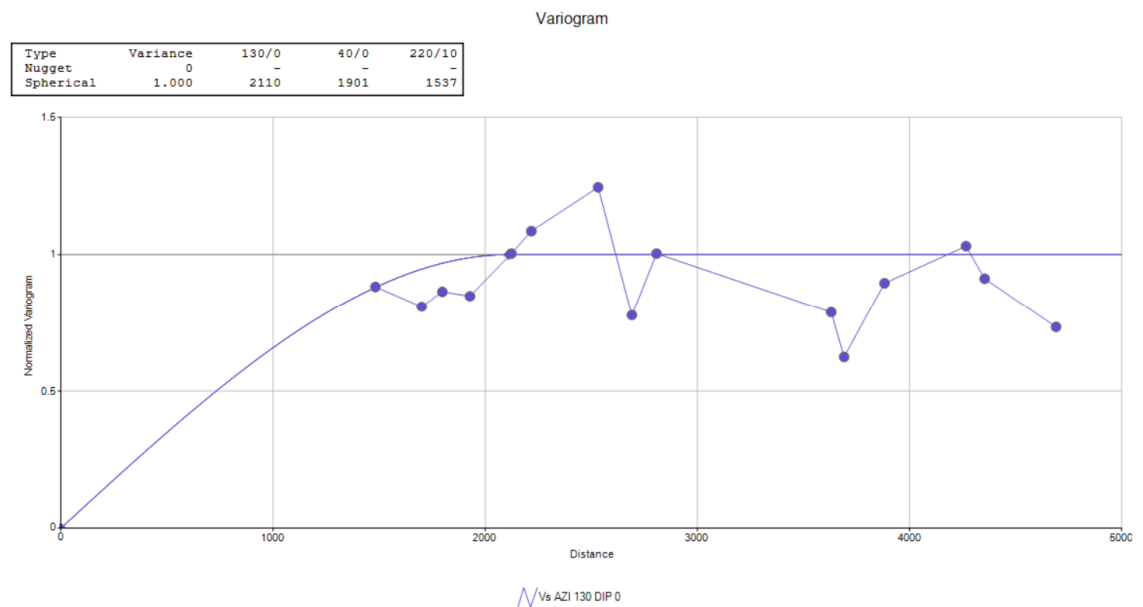


Figure 9. Variogram model for shear wave velocity in azimuth 130 and dip 0.

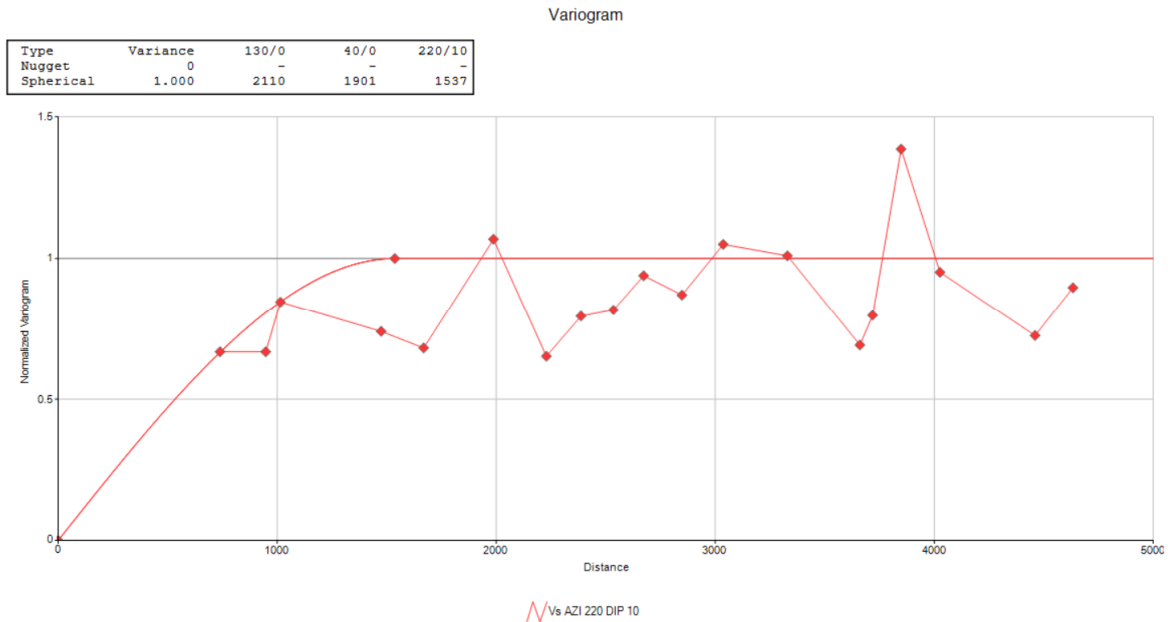


Figure 10. Variogram model for shear wave velocity in azimuth 220 and dip 10.

As formerly mentioned, the variogram parameters are crucial information for 3D geostatistical modeling. These parameters have been acquired through the best fitted theoretical variogram model (see Figures 8-10). According to Figures 8-10, the best theoretical variogram model fitted in 3 perpendicular direction is spherical model, and other characteristics of the variogram such as azimuth, dip, search radius, sill and nugget effect have been shown on the top and the bottom of variograms.

5.2.2. Cross validation

After determining the variogram models, Cross-Validation has been used to validate variogram models. In this approach, estimates are compared with the measured values for a collection of sites different from those used as input data [47]. Cross-validation (which is also known as jack-knifing or point kriging) is sometimes used in an attempt to determine the “best” variogram model to use in the grade estimation process. Also, kriging plans are

sometimes optimized based on cross validation exercises. The most commonly used requiring that a sample be extracted from the database and its value re-estimated using the remaining samples and the variogram models being tested. This method requires using a well-established stationary domain with a good number of samples, such that about 50 % of them can be taken out and still the variogram model and other statistical properties are maintained [50]. The XVALID process provides a statistical method of fitting variogram parameters. Each sample in the data set is removed in turn and its value is estimated from the remaining data using point kriging. Thus for each sample there is an actual value and a kriged value estimated from the surrounding data. The XVALID process calculates a set of statistics comparing actuals and estimates which show how good (or bad) the estimates are [51]. The scatter plot of actual shear wave velocity versus the estimated values have been shown in Figure 11. Furthermore, the cross validation statistics are presented in Table 2.

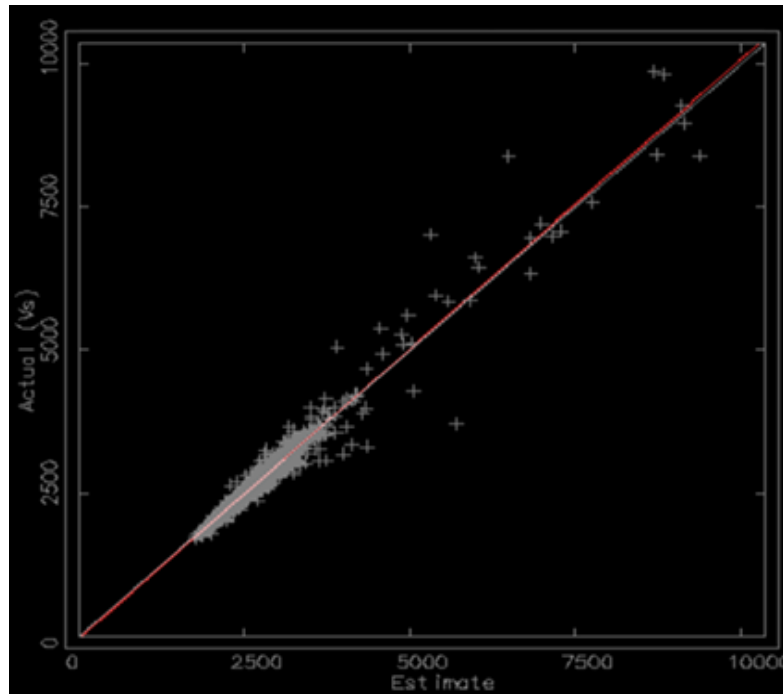


Figure 11: Scatter plot of actual shear wave velocity versus the estimated values.

Figure 11 shows that there is a significant correlation of determinations ($R=0.994$; see Table 2) between the actual shear wave velocity and the estimated values. The result of this figure shows

that the accuracy of the estimated values from this approach is extremely acceptable. For further checking, the cross-validation statistics have been shown in Table 2.

Table 2. Cross-validation statistics for shear wave velocity.

Number of samples estimated	36477
Number of samples not estimated	30
Mean of actual values	2757.64465
Mean of estimated values	2757.61814
Mean difference (Act-Est)	0.02651131
Mean difference (as % of actual)	0
Mean absolute difference	14.6445387
Variance of actual values	111005.615
Variance of estimated values	107425.813
Correlation coefficient	0.994
Kriging variance: mean of KV estimated from model	0.00015548
Kriging variance: mean of squared differences	1259.53894
Kriging variance: ratio	0

Table 2 demonstrates the remarkable results for a number of samples, mean difference, correlation coefficient, and Kriging variance estimated by the jackknife Kriging approach. Finally, the results of this approach show that the elliptical search area by those variograms are highly accurate in any points of the reservoir in the oil field for estimating the shear wave velocity.

5.2.3. 3D Model by Ordinary Kriging Estimator

After finding the perfect elliptical search area based on the variography parameters obtained from the perpendicular variogram, the 3D model of shear wave velocity was constructed by utilizing the OK estimator. This process was carried out in the Datamine software. Therefore, at first, the datasets in 30 wells, obtained from the empirical

correlation, were used as the input data, and then the block model for overall reservoir was constructed (the block size was 200, 300, and 15 m). Ultimately, the shear wave velocity for each block was estimated using the elliptical search area

and OK estimator. Figure 12 shows the result of estimation shear wave velocity for every block in the whole reservoir of the oil field by the OK estimator.

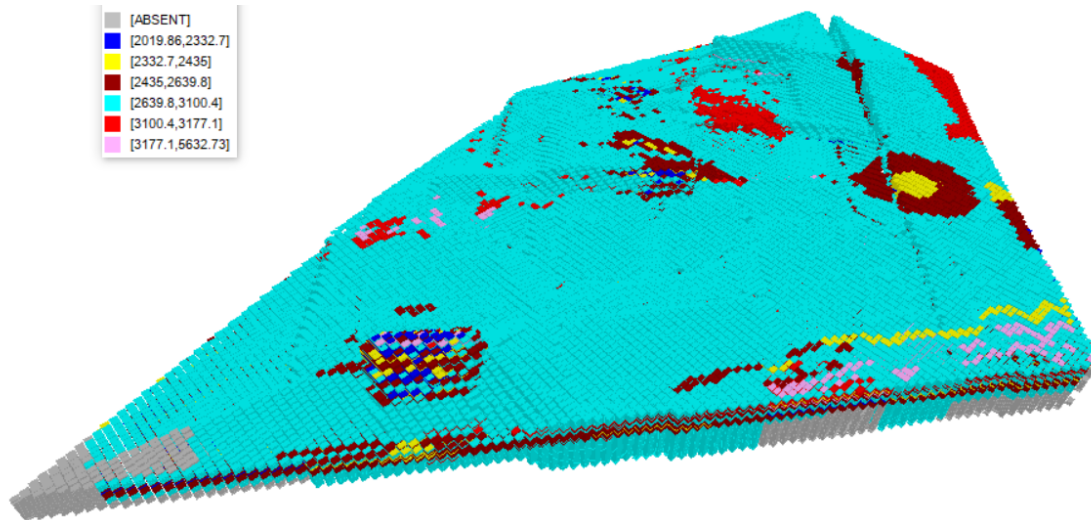


Figure 12. Estimation of shear wave velocity (3D model) by utilizing OK estimator in the whole of reservoir oil field.

Figure 12 shows the 3D model for shear wave velocity that has been estimated by the OK estimator. In some points, this estimator has not been able to obtain a value for the favorable block (see the absent block with gray color in Figure 12). In this 3D model, the absent block from shear wave velocity is due to the low radius for the elliptical search area. Furthermore, the shear wave velocity in the other blocks estimated by the OK estimator is shown in 6 ranges with 6 different colors. These 6 ranges for shear wave velocity were determined by the cumulative frequency. The 3D shear wave model in this case study was considered as a key information about the reservoir oil field that could be used to make a 3D geomechanics model, although it may not be accurate. Therefore, in order

to evaluate the accuracy of the 3D shear wave velocity model, the reliability of the estimated values was verified.

5.2.4. Reliability of estimated values

In geostatistics, Kriging variance (KVar) has been used to measure the reliability of the estimated values (see section 4.2 for more information). Therefore, the KVar has been utilized to measure the error of the estimation by OK estimator for understanding the reliability of the estimated values. The estimation variance of shear wave velocity by KVar was determined and shown as a distribution 3D block model for the overall reservoir of oil field in Figure 13.

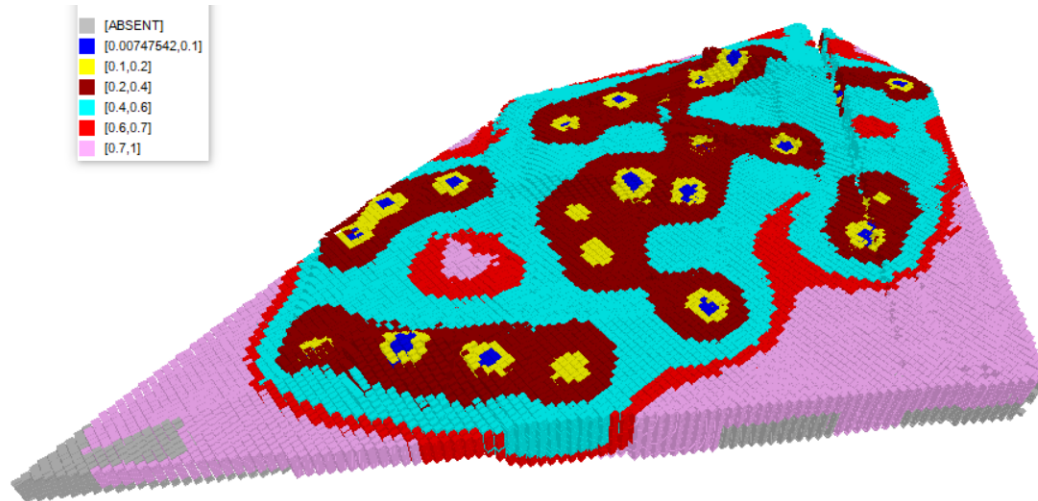


Figure 13. 3D block model of Kriging estimation variance in the whole of reservoir oil field.

Figure 13 shows the 3D errors block model for estimating the shear wave velocity by the OK estimator. For standardization of the data, the estimation variance values are between 0 and 1. The minimum values of the estimation variance indicated that the errors of estimation of the shear wave velocities by the OK estimator were minimum. Furthermore, the enhancement estimation variance indicated that the error of estimator increased. According to this declaration for the results of the 3D KVar, the minimum errors are around the drilled boreholes that the shear wave velocities were available, and also away from around the drilled boreholes that the error estimation increased. Furthermore, the 3D block model of KVar is shown in 6 ranges with 6 different colors, which were determined by the cumulative frequency. Finally, those results show that the estimated values by the OK estimator are strongly acceptable, and accurate for this case study.

6. Conclusions

In this research work, the magnitude of shear wave velocity was estimated using two different techniques including the Back-Propagation Neural Network (BPNN) and Ordinary Kriging (OK) together with the conventional petrophysics logs. Our findings illustrated that the BPNN technique presented an extremely low correlation coefficient ($R = 0.32$) with a high error, and consequently, it was not able to accurately estimate the values of shear wave velocity. The potential rationale for this drawback is that while the BPNN technique is an extrapolation method, the changes in the subsurface geomechanical conditions are mainly

intense in the oil reservoirs. To the contrary, through the OK technique, a new 3D model for estimating the shear wave velocity was acquired so that it presented a high correlation coefficient, and also was acutely accurate. Such a high accuracy is perhaps derived from this point that the OK technique is based on an interpolation approach. Therefore, it can be expressed that the OK technique is substantially a more reliable estimator than the BPNN technique for determination of the shear wave velocities in the oil reservoirs. Furthermore, the results obtained indicated that in the absence of the DSI logs, the values of shear wave velocity could be estimated by utilization of the conventional petro-physics well logs. The results obtained from the affordable and acceptable 3D geostatistics model could be utilized to estimate the shear wave velocities throughout the subjected oil reservoir in the current research work. More than this, such a geostatistics model could also be applied to any other oil field containing reservoirs with identical geological and geomechanical characteristics.

References

- [1]. Pickett, G.R. (1963). Acoustic character logs and their applications in formation evaluation. *Journal of Petroleum technology*. 15 (06): 659-667.
- [2]. Carroll, R.D. (1969). The determination of the acoustic parameters of volcanic rocks from compressional velocity measurements. In *International Journal of Rock Mechanics and Mining Sciences & Geomechanics Abstracts*. 6 (6): 557-579.
- [3]. Tosaya, C., and Nur, A. (1982). Effects of diagenesis and clays on compressional velocities in rocks. *Geophysical Research Letters*. 9 (1): 5-8.

- [4]. Domenico, S.N. (1984). Rock lithology and porosity determination from shear and compressional wave velocity. *Geophysics*. 49 (8): 1188-1195.
- [5]. Castagna, J.P., Batzle, M.L., and Eastwood, R.L. (1985). Relationships between compressional-wave and shear-wave velocities in clastic silicate rocks. *geophysics*,. 50 (4): 571-581.
- [6]. Han, D.H., Nur, A., and Morgan, D. (1986). Effects of porosity and clay content on wave velocities in sandstones. *Geophysics*. 51 (11): 2093-2107.
- [7]. Eissa, E.A., and Kazi, A. (1988). Relation between static and dynamic Young's moduli of rocks. *International Journal of Rock Mechanics and Mining & Geomechanics Abstracts*. 25 (6): 479-482.
- [8]. Boonen, P., Bean, C., Tepper, R., and Deady, R. (1998, May). Important Implications From A Comparison Of Lwd And Wireline Acoustic Data From A Gulf Of Mexico Well. In *SPWLA 39th Annual Logging Symposium*. OnePetro, 1-14.
- [9]. Krief, M., Garat, J., Stellingwerff, J., and Ventre, J. (1990). A petrophysical interpretation using the velocities of P and S waves (full-waveform sonic). *The Log Analyst*, 31(06).
- [10]. Anselmetti, F.S., and Eberli, G. P. (1993). Controls on sonic velocity in carbonates. *Pure and Applied geophysics*. 141 (2): 287-323.
- [11]. Yasar, E., and Erdogan, Y. (2004). Correlating sound velocity with the density, compressive strength and Young's modulus of carbonate rocks. *International Journal of Rock Mechanics and Mining Sciences*. 41 (5): 871-875.
- [12]. Brocher, T.M. (2005). Empirical relations between elastic wave speeds and density in the Earth's crust. *Bulletin of the seismological Society of America*. 95 (6): 2081-2092.
- [13]. Ameen, M.S., Smart, B.G., Somerville, J.M., Hammilton, S., and Naji, N.A. (2009). Predicting rock mechanical properties of carbonates from wireline logs (A case study: Arab-D reservoir, Ghawar field, Saudi Arabia). *Marine and Petroleum Geology*. 26 (4): 430-444.
- [14]. Wadhwa, R.S., Ghosh, N., and Subba-Rao, C. (2010). Empirical relation for estimating shear wave velocity from compressional wave velocity of rocks. *Journal of Indian Geophysical Union*. 14 (1): 21-30.
- [15]. Rasouli, V., Pallikathekathil, Z.J., and Mawuli, E. (2011). The influence of perturbed stresses near faults on drilling strategy: a case study in Blacktip field, North Australia. *Journal of Petroleum Science and Engineering*. 76(1-2), 37-50.
- [16]. Zhang, W., Ma, Q., Wang, R., and Ren, S. (2011). An experimental study of shear strength of gas-hydrate-bearing core samples. *Petroleum Science*. 8 (2): 177-182.
- [17]. Maleki, S.h., Moradzadeh, A., Riabi, R.G., Gholami, R., and Sadeghzadeh, F. (2014). Prediction of shear wave velocity using empirical correlations and artificial intelligence methods. *NRIAG Journal of Astronomy and Geophysics*. 3 (1): 70-81.
- [18]. Bagheripour, P., Gholami, A., Asoodeh, M., and Vaezzadeh-Asadi, M. (2015). Support vector regression based determination of shear wave velocity. *Journal of Petroleum Science and Engineering*, 125, 95-99.
- [19]. Behnia, D., Ahangari, K., and Moeinossadat, S.R. (2017). Modeling of shear wave velocity in limestone by soft computing methods. *International Journal of Mining Science and Technology*. 27 (3): 423-430.
- [20]. Rezaee, M.R., Ilkhchi, A.K., and Barabadi, A. (2007). Prediction of shear wave velocity from petrophysical data utilizing intelligent systems: An example from a sandstone reservoir of Carnarvon Basin, Australia. *Journal of Petroleum Science and Engineering*. 55 (3-4): 201-212.
- [21]. Rajabi, M., Bohloli, B., and Ahangar, E.G. (2010). Intelligent approaches for prediction of compressional, shear and Stoneley wave velocities from conventional well log data: A case study from the Sarvak carbonate reservoir in the Abadan Plain (Southwestern Iran). *Computers & Geosciences*. 36 (5): 647-664.
- [22]. Ghorbani, A., Jafarian, Y., and Maghsoudi, M.S. (2012). Estimating shear wave velocity of soil deposits using polynomial neural networks: Application to liquefaction. *Computers & Geosciences*, 44, 86-94.
- [23]. Nourafkan A. and Kadkhodaie-Ilkhchi A. (2015). Shear wave velocity estimation from conventional well log data by using a hybrid ant colony-fuzzy inference system: A case study from Cheshmeh-Khosh oilfield. *Journal of Petroleum Science and Engineering*. 127: 459-468.
- [24]. Anemangely, M., Ramezanzadeh, A., and Tokhmechi, B. (2017). Shear wave travel time estimation from petrophysical logs using ANFIS-PSO algorithm: A case study from Ab-Teymour Oilfield. *Journal of Natural Gas Science and Engineering*, 38, 373-387.
- [25]. Tercan, A.E., and Özçelik, Y. (2000). Geostatistical evaluation of dimension-stone quarries. *Engineering Geology*. 58 (1): 25-33.
- [26]. Marinoni, O. (2003). Improving geological models using a combined ordinary-indicator kriging approach. *Engineering geology*. 69 (1-2): 37-45.
- [28]. Deng, M. G., Li, W. C., Bo, L.I., Li, L. H., Jiang, S.D., Xiong, G.X., and Yu, H.J. (2007). Application of Log Kriging on estimated reserves of the 10-9 ore body of Lutangba in the Gejiu Tin deposits. *Journal of China University of Mining and Technology*. 17 (2): 286-289.
- [29]. Daya A.A. (2012). Reserve estimation of central part of Choghart north anomaly iron ore deposit through

ordinary kriging method. *International Journal of Mining Science and Technology*. 22 (4): 573-577.

[30]. Mohammadi, S.S., Hezarkhani, A. and Tercan, A. E. (2012). Optimally locating additional drill holes in three dimensions using grade and simulated annealing. *Journal of the Geological Society of India*. 80 (5): 700-706.

[31]. Doostmohammadi, M., Jafari, A., and Asghari, O. (2015). Geostatistical modeling of uniaxial compressive strength along the axis of the Behesht-Abad tunnel in Central Iran. *Bulletin of Engineering Geology and the Environment*. 74 (3): 789-802.

[32]. Nazari-Ostad M., Asghari O., Emery X., Azizzadeh M. and Khoshbakht F. (2016). Fracture network modeling using petrophysical data, an approach based on geostatistical concepts. *Journal of Natural Gas Science and Engineering*, 31, 758-768.

[33]. Rahimi, H., Asghari, O., and Hajizadeh, F. (2018). Selection of optimal thresholds for estimation and simulation based on indicator values of highly skewed distributions of ore data. *Natural Resources Research*. 27 (4): 437-453.

[34]. Nezhad, Y.A., Moradzadeh, A., and Kamali, M.R. (2018). A new approach to evaluate Organic Geochemistry Parameters by geostatistical methods: A case study from western Australia. *Journal of Petroleum Science and Engineering*, 169, 813-824.

[35]. Waller, L.A., and Gotway, C.A. (2004). *Applied spatial statistics for public health data* (Vol. 368). John Wiley & Sons.

[36]. Webster, R., and Oliver, M.A. (2007). *Geostatistics for environmental scientists*. John Wiley & Sons.

[37]. Armstrong, M. (1998). *Basic linear geostatistics*. Springer Science & Business Media.

[38]. Shahbeik, S., Afzal, P., Moarefvand, P., and Qumarsy, M. (2014). Comparison between ordinary kriging (OK) and inverse distance weighted (IDW) based on estimation error. Case study: Dardevey iron ore deposit, NE Iran. *Arabian Journal of Geosciences* 7 (9): 3693-3704.

[39]. Afzal, P. (2018). Comparing ordinary kriging and advanced inverse distance squared methods based on estimating coal deposits; case study: East-Parvadeh

deposit, central Iran. *Journal of Mining and Environment*. 9 (3): 753-760.

[40]. James, G. A., and Wynd, J. G. (1965). Stratigraphic nomenclature of Iranian oil consortium agreement area. *AAPG bulletin*. 49 (12): 2182-2245.

[41] Sadooni, F.N. (1993). Stratigraphic Sequence, Microfacies, and Petroleum Prospects of the Yamama Formation, Lower Cretaceous, Southern Iraq. *AAPG bulletin*. 77 (11): 1971-1988.

[42]. Narendra K.S. and Parthasarathy K. (1990). Identification and control of dynamical systems using neural networks. *IEEE Transactions on neural networks*. 1 (1): 4-27.

[43]. Haykin, S. (1994). *Neural networks: A comprehensive foundation*, prentice hall ptr. Upper Saddle River, NJ, USA.

[44]. Deutsch, C.V., and Hewett, T.A. (1996). Challenges in reservoir forecasting. *Mathematical geology*. 28 (7): 829-842.

[45]. Hohn, M. (1998). *Geostatistics and petroleum geology*. Springer Science & Business Media.

[46]. Pyrcz, M.J., and Deutsch, C.V. (2014). *Geostatistical reservoir modeling*. Oxford university press.

[47]. Mostafaei, K., and Ramazi, H.R. (2018). 3D model construction of induced polarization and resistivity data with quantifying uncertainties using geostatistical methods and drilling (Case study: Madan Bozorg, Iran). *Journal of Mining and Environment*. 9 (4): 857-872.

[48]. Gotawala, D.R., and Gates, I.D. (2010). On the impact of permeability heterogeneity on SAGD steam chamber growth. *Natural Resources Research*. 19 (2): 151-164.

[49]. Zawadzki, J., and Fabijańczyk, P. (2007). Use of variograms for field magnetometry analysis in Upper Silesia Industrial Region. *Studia Geophysica et Geodaetica*. 51 (4): 535-550.

[50]. Rossi, M.E., and Deutsch, C.V. (2014). *Mineral resource estimation*. Dordrecht: Springer Science & Business Media.

[51]. Deutsch, C.V., and Journel, A.G. (1992). *Geostatistical software library and user's guide*. New York. 119 (147).

ارائه یک مدل سه بعدی جدید برای تخمین سرعت موج برشی از طریق نگاره‌های پتروفیزیکی و روش زمین آمار

شاهو ملکی^۱، حمیدرضا رمضی^{۱*} و محمدجواد عامری شهرابی^۲

۱- بخش مهندسی معدن و متالورژی، دانشگاه صنعتی امیرکبیر، ایران

۲- بخش مهندسی نفت، دانشگاه صنعتی امیرکبیر، ایران

ارسال ۲۰۲۲/۱۲/۰۷، پذیرش ۲۰۲۲/۰۳/۰۸

* نویسنده مسئول مکاتبات: ramazi@aut.ac.ir

چکیده:

سرعت موج برشی (V_s) همیشه به عنوان یکی از پارامترهای کلیدی در تعیین خواص زیر سطحی ژئومکانیکی مخازن هیدروکربوری بوده است. در خلال عملیات چاه نگاری، مقدار V_s را می‌توان بصورت مستقیم از طریق نگار صوتی دوقطبی (DSI) اندازه گیری کرد. از نقاط ضعف این روش می‌توان علاوه بر تفسیر یک بعدی آن به هزینه بالای انجام کار اشاره کرد. از اینرو، در این تحقیق تلاش گردید روش جایگزینی برای تخمین سرعت موج برشی از طریق نگاره‌های متداول پتروفیزیکی مانند سرعت موج فشاری (V_p) در یک مطالعه موردی در یکی از مخازن کربناته در جنوب ایران ارائه داده شود. برای انجام کار، در ابتدا سرعت موج برشی واقعی یک مجموعه داده در یک چاه در میدان مورد نظر بکار گرفته شد. همبستگی بین سرعت موج فشاری و موج برشی واقعی این مجموعه داده که از نگار صوتی دو قطبی بود استخراج گردید. سپس رابطه بدست آمده از همبستگی موجود برای دیگر چاه‌ها که سرعت موج فشاری آن‌ها وجود داشت و حدود سی چاه بود استفاده گردید و برای آن‌ها سرعت موج برشی شان تخمین زده شد. در ادامه روش تخمینگر کریجینگ همراه با شبکه عصبی برگشتی (BPNN) برای محاسبه سرعت موج برشی در سرتاسر مخزن هیدروکربوری بکار گرفته شد. نتایج بدست آمده از این دو تکنیک با یکدیگر مقایسه گردید که نشان داده روش تخمین کریجینگ مقادیر و مدل بسیار دقیق‌تری ارائه داده است. نتایج این تحقیق نشان داد کاربرد روش تخمینگر کریجینگ نسبت به شبکه عصبی برگشتی برای تخمین سرعت موج برشی بسیار دقیق و قابل اعتمادتر خواهد بود و مدل بدست آمده در میادین مشابه که شرایط ژئومکانیکی و زمین شناسی نزدیکی با این تحقیق داشته باشد کارا و مناسب خواهد بود.

کلمات کلیدی: مدل سه بعدی، تخمین، تخمینگر کریجینگ، نگاره‌های چاه، سرعت موج برشی.